ACCOUNTS of chemical research

Article

pubs.acs.org/accounts

Decoupling Interrelated Parameters for Designing High Performance Thermoelectric Materials

Chong Xiao, Zhou Li, Kun Li, Pengcheng Huang, and Yi Xie*

Hefei National Laboratory for Physical Sciences at the Microscale and Collaborative Innovation Center of Chemistry for Energy Materials, University of Science and Technology of China, Hefei, Anhui 230026, People's Republic of China

ABSTRACT: The world's supply of fossil fuels is quickly being exhausted, and the impact of their overuse is contributing to both climate change and global political unrest. In order to help solve these escalating problems, scientists must find a way to either replace combustion engines or reduce their use.

Thermoelectric materials have attracted widespread research interest because of their potential applications as clean and renewable energy sources. They are reliable, lightweight, robust, and environmentally friendly and can reversibly convert between heat and electricity. However, after decades of development, the energy conversion efficiency of thermoelectric devices has been hovering around 10%. This is far below the theoretical predictions, mainly due to the interdependence and coupling between electrical and thermal parameters, which are strongly interrelated through the electronic structure of the materials. Therefore, any strategy that balances or decouples these parameters, in addition to optimizing the materials' intrinsic electronic structure, should be critical to the development of thermoelectric technology.

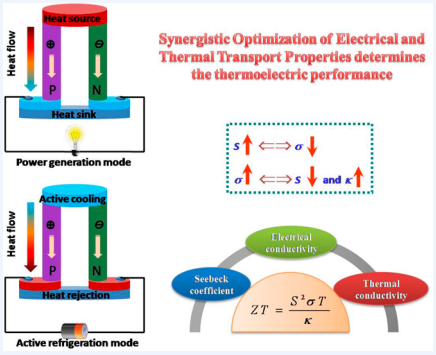

In this Account, we discuss our recently developed strategies to decouple thermoelectric parameters for the synergistic optimization of electrical and thermal transport. We first highlight the phase transition, which is accompanied by an abrupt change of electrical transport, such as with a metal−insulator and semiconductor−superionic conductor transition. This should be a universal and effective strategy to optimize the thermoelectric performance, which takes advantage of modulated electronic structure and critical scattering across phase transitions to decouple the power factor and thermal conductivity. We propose that solid-solution homojunction nanoplates with disordered lattices are promising thermoelectric materials to meet the "phonon glass electron crystal" approach. The formation of a solid solution, coupled with homojunctions, allows for synergistically enhanced thermoelectric properties. This occurs through a significant reduction of thermal conductivity, without the deterioration of thermopower and electrical conductivity. In addition, we introduce the concept of spin entropy in wide band gap semiconductor nanocrystals, which acts to fully disentangle the otherwise interconnected quantities for synergistically optimized thermoelectric performance. Finally, we discuss a new concept we developed that is based on an ultrathin-nanosheet composite that we fabricated from ultrathin nanosheets of atomic thickness. These retain the original strong two-dimensional electron gas (2DEG) and allow for decoupled optimization of the three thermoelectric parameters, which improves thermoelectric performance.

1. INTRODUCTION

Because of the dramatic escalation of social and political unrest as well as increasing environmental deterioration caused by the demand and combustion of fossil fuels,[1,2] thermoelectric materials have attracted widespread research interest in potential applications for clean and renewable energy sources, which may provide an optimized solution for improving energy efficiency and mitigating environment issues, due to their capability of reversibly converting between heat and electricity with the advantages of being reliable, lightweight, robust, and environmentally friendly.[3−13]

The performance of thermoelectric materials is quantified by a dimensionless figure of merit, ZT, which is defined as $ZT = S^2\sigma T/\kappa$, where S is the Seebeck coefficient, that is, the thermoelectric power, σ is the electrical conductivity, T is the absolute temperature, and κ is the thermal conductivity. As seen in Figure 1, this ZT value determines the energy conversion efficiency of thermoelectric materials:

$$\eta = \frac{T_h - T_c}{T_h}\frac{\sqrt{1+ZT}-1}{\sqrt{1+ZT}+T_c/T_h} \quad (1)$$

where the η is energy conversion efficiency and T_h and T_c are the hot side and cold side temperature, respectively. In the thermoelectric community, the consensus is that ZT = 1 is a benchmark for practical applications, which has been the barrier for more than 50 years. Further, it is expected that on attainment of ZT = 3, the energy conversion efficiency of thermoelectric materials will be sufficient for the general replacement of traditional power generation and refrigerating devices by thermoelectric units. Though there is no theoretical limit to the values of ZT, the ability to design thermoelectric materials with ZT approaching the above targeted value has

Received: December 4, 2013
Published: February 11, 2014

   dx.doi.org/10.1021/ar400290f | Acc. Chem. Res. 2014, 47, 1287−1295

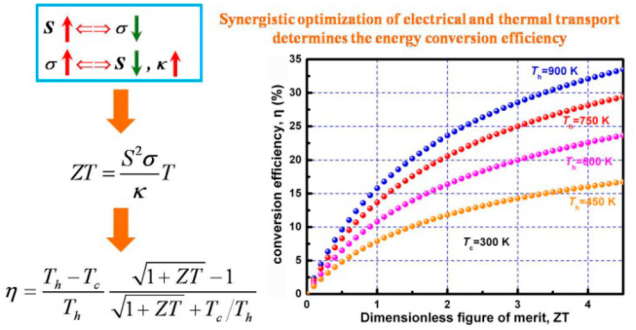

Figure 1. Conversion efficiency of thermoelectric materials at different ZT value and hot side temperature (T_h). The cold side temperature (T_c) is 300 K. These curves are calculated under the assumption that ZT is constant versus temperature.[17]

proven extremely difficult, which is mainly because of the strongly interrelated thermoelectric parameters.

Boltzmann transport theory describes both electrical and thermal transport in the vast majority of solids. This theory provides a general understanding of the Seebeck coefficient and electrical conductivity, which is expressed in the eqs 2 and 3:[14,15]

$$S = \frac{8\pi^2 k_B^2}{3eh^2} m^* T \left(\frac{\pi}{3n}\right)^{2/3} \quad (2)$$

$$\sigma = ne\mu \quad (3)$$

where k_B is the Boltzmann constant, e is the carrier charge, h is Planck's constant, m^* is the effective mass of the charge carrier, n is the carrier concentration, and μ is the carrier mobility. Meanwhile, the Wiedemann–Franz law describes that the total thermal conductivity is the sum of two independent components, a lattice contribution, κ_l and an electronic contribution κ_e. According to the Wiedemann–Franz law, κ_e is expressed in eq 4:[16]

$$\kappa_e = L\sigma T \quad (4)$$

where L is the Lorentz number, typically taken as 2.45×10^{-8} $W{\cdot}\Omega{\cdot}K^{-2}$ in materials having a highly degenerate electron gas. So, as seen from eqs 1, 2 and 3, it is clear that the three thermoelectric parameters are strongly interrelated and often follow unfavorable opposing trends, which impedes the significant improvement of ZT value. Therefore, any strategy based on the decoupling or balancing of these three parameters for synergistic optimization of electrical and thermal transport to substantially improve the performance of thermoelectric materials should be highly desirable for the breaking of their low energy conversion efficiency constraints in the practical applications.

In this Account, we focus on our recently developed new strategies: phase transition with abrupt change of electrical conductivity, superionic conductor with disordered structure, spin entropy in wide-gap semiconductors, and atomically thick ultrathin nanosheets with 2D electron gas to synergistically optimize electrical and thermal transport to achieve significantly improved thermoelectric performance. We present our recent work in these directions and put it in light of the literature.

2. DECOUPLING OF POWER FACTOR AND THERMAL CONDUCTIVITY

According to the Boltzmann transport theory and Wiedemann–Franz law, the lattice contribution to the thermal conductivity, κ_l, is independent of the electrical conductivity, which implies that the combination of the enhancement of power factor ($S^2\sigma$) and reduction of lattice thermal conductivity should be the most effective strategy for the acquisition of high performance thermoelectric materials. The power factor is a purely electronic property, dominated by the details of the electronic band structure. Meanwhile, the lattice thermal conductivity in solids is governed by phonons, which is the dissipation of vibrational energy between adjacent atoms through chemical bonding. Since the band structure and chemical bonding of many semiconductors used in the thermoelectric converters are related to their crystal structure, the above-mentioned power factor and thermal conductivity can be simultaneously optimized through the variation of crystallography parameters.

2.1. Phase Transition with Abrupt Change of Electronic Structure and Critical Scattering of Phonons

Occurrence of different polymorphic phases has often been observed in inorganic compounds, especially in synthetic materials.[18] Among them, many exhibit transformations from one crystal structure to another as the temperature or pressure is varied, which is the so-called phase transition. During such phase transitions, the involved changes in atomic configuration should acutely fluctuate the sample density, which results in enhanced phonon scattering to optimize the thermal conductivity. At the same time, besides the changes in atom arrangement, many of the solids also experience changes in the electronic structure, which has revealed to us an intriguing route to modulate the electronic structure and carrier transport properties through phase transition.[19]

VO_2, a typical strongly electron–electron correlated system, is the first example to realize optimized thermoelectric performance through the phase transition modulating electrical and thermal transport properties.[20] As is known, monoclinic VO_2(M) (room-temperature phase, <340 K) and rutile VO_2(R) (nonambient phase, >340 K) are typical states in a temperature-driven, fully reversible structural phase-transition process. As seen in Figure 2, in the rutile VO_2(R), the isometric V–V bond (2.88 Å) results in the itinerant 3d electrons in the overlapped V 3d orbitals, leading to the electrically conducting state. In the monoclinic VO_2(M), the V–V bond splits into alternately altered bond lengths of 2.62 and 3.16 Å; thus the outer V 3d electrons are localized, which results in the electrically insulated.[21,22] These electronic structure transformations enable the phase transition be used to effectively regulate the carrier transport properties and optimize the thermoelectric property: the ZT value reaches the maximum during the process of phase transition.

Inspired by the strategy of controlling the carrier concentrations in the material system with phase transition behavior, other kinds of materials with intrinsic phase transition also show promising signs for tailoring the optimal thermoelectric performance. Thanks to their intrinsic reversible transformation between semiconductor and superionic conductor, silver chalcogenides have attracted tremendous interests.[23−25] For example, Ag_2Se[26] crystallizes in the orthorhombic phase with two crystallographically distinct silver atoms at room temperature, behaving as a narrow band gap

dx.doi.org/10.1021/ar400290f | Acc. Chem. Res. 2014, 47, 1287−1295

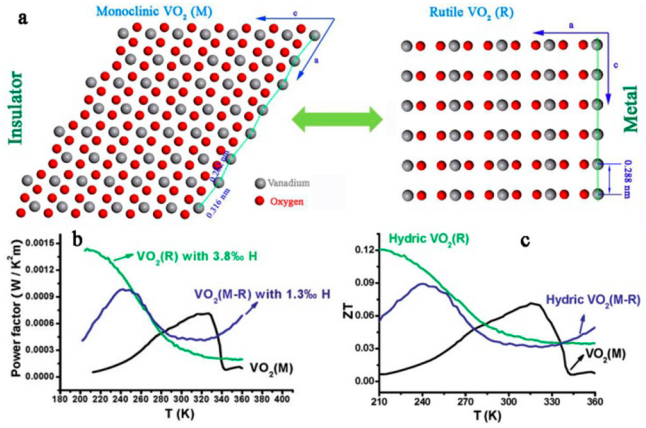

Figure 2. (a) Schematic illustration of the metal and insulator states by different alignment styles of vanadium atoms in vanadium oxides. Temperature dependence of the power factor (b) and thermoelectric figure of merit (c) in hydric VO_2(R), VO_2(M), and hydric VO_2(M–R). Panels b and c were adapted with permission from ref 20. Copyright 2011 American Chemical Society.

semiconductor, while at high temperature, Ag_2Se is cubic phase and silver atoms are statistically distributed over several interstitial sites of the selenium sublattice, through which Ag^+ ions can move easily and show superionic conductivity. These two compounds undergo a reversible first-order phase transition around 406 K with a remarkable change in its electric property, which is presently giving a hint for the modulation of the electric properties at the phase transition temperature to optimize the thermoelectric power factor.[27] On the other hand, by combination of the adequate grain boundary of nanocrystals, the lattice distortion during the phase transition and the Ag^+ ion disordering, an ultralow value of thermal conductivity is successfully retained over the whole investigated temperature range. As a consequence, a maximized ZT is achieved around the temperature of the semiconductor–superionic conductor transition (as seen in Figure 3).

Recently, the significantly improved thermoelectric performance in accordance with modulated electrical and thermal transport properties through electron and phonon critical scattering during the phase transition has also been reported in Cu_2Se, which shows a dramatically increased ZT value of 2.3 at

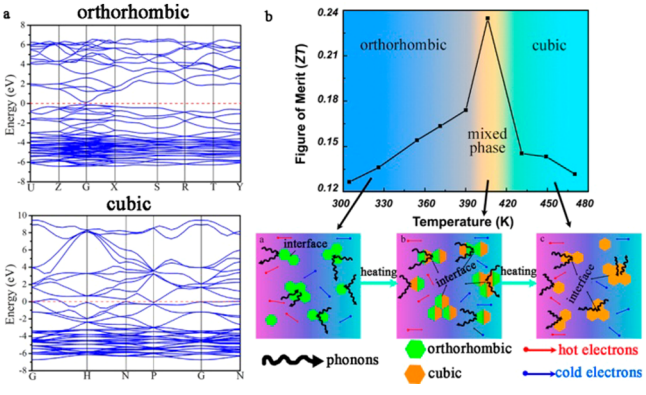

Figure 3. (a) Band structure of orthorhombic and cubic Ag_2Se and (b) thermoelectric properties of Ag_2Se nanocrystals and schematic representation of phonon scattering mechanisms during the phase transition. Adapted with permission from ref 27. Copyright 2012 American Chemical Society.

400 K (as seen in Figure 4).[28] At low temperature, α-Cu_2Se has a lower symmetry crystal structure, where the Cu atoms are

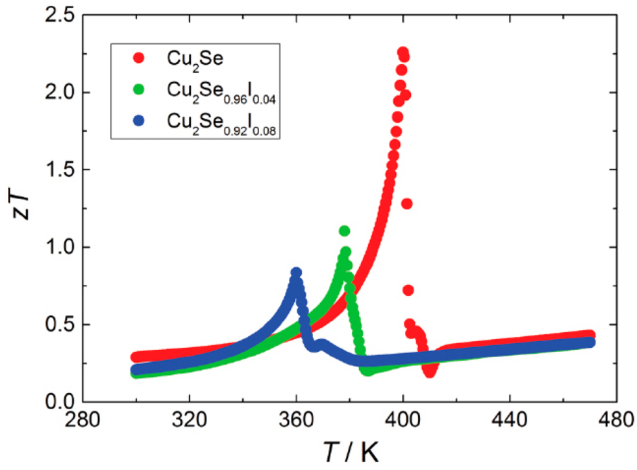

Figure 4. ZT curves for iodine-doped Cu_2Se, which show hugely increased values due to electron and phonon critical scattering during the phase transition. Adapted with permission from ref 28. Copyright 2013 Wiley-VCH.

localized. As the temperature increases to 400 K, α-Cu_2Se transforms into cubic phase (β-Cu_2Se), in which Cu^+ ions are kinetically disordered throughout the Se atoms forming face-centered cubic (fcc) structure. During this phase transition, the violent fluctuations of structure, chemical composition, and density result in a strong critical scattering of carriers and phonons to achieve very high thermopower and low thermal conductivity and thereby exceptional thermoelectric performance. Furthermore, with iodine doping, the critical phase transition temperature, accompanying the maximum of ZT values can be tuned to within a few tens of degrees around room temperature. All above-mentioned exciting experimental results undoubtedly reveal that regulating the phase transition behavior in solids allows advances in balancing the electric and thermal properties for optimal thermoelectric performance.

In addition to the optimized electrical and thermal transport properties in the phase transition system, we also found that the dimetal chalcogenides show more sophisticated and unexpected properties, which integrate high thermoelectric performance and reversible p–n–p semiconducting switching (as seen in Figure 5).[29] For example, $AgBiSe_2$ is a p-type semiconductor and crystallizes in hexagonal phase at room temperature. As the temperature increases, $AgBiSe_2$ is observed to undergo continuous phase transition to rhombohedral phase around 410 K and then to cubic phase around 580 K.[30,31] During the thermal disorder process, Ag/Bi atom exchange via Ag vacancies results in a quasi-metallic state bringing more conduction valence electrons, which eventually leads to the switching between p- and n-type conduction. Likewise, a maximum ZT value is obtained at the phase transition temperature, which is similar to that of Ag_2X (X = S, Se). On the other hand, high disordering of Ag/Bi atoms in cubic phase at high temperature causes much stronger anharmonicity of the chemical bond and drives the phonon–phonon umklapp scattering, which could significantly reduce the lattice thermal conductivity and simultaneously show high electric conductivity due to the high mobility of these disordering ions, resulting in high thermoelectric performance at high temperature.

dx.doi.org/10.1021/ar400290f | Acc. Chem. Res. 2014, 47, 1287–1295

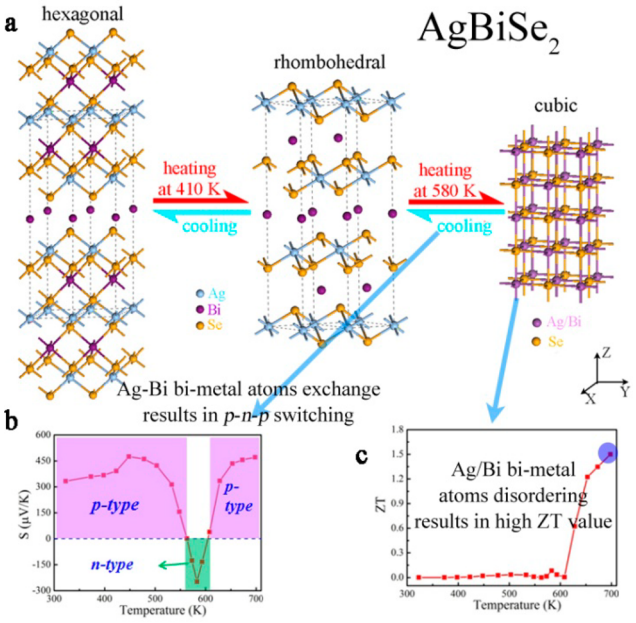

Figure 5. (a) Crystal structural evolution of $AgBiSe_2$ among the hexagonal, rhombohedral, and cubic phase. Temperature dependences of Seebeck coefficient S (b) and dimensionless figure-of-merit ZT (c) of $AgBiSe_2$. A pronounced peak in the Seebeck coefficient with two changes in the sign of the value was observed. Adapted with permission from ref 29. Copyright 2012 American Chemical Society.

2.2. Spin-State Transition

In addition to the structural phase transition, the spin-state transition was also found to induce the optimization of thermoelectric performance. Taking Ce-doped $LaCoO_3$ as an example,[32] the charge transport depends strongly on the spin-state of the background Co^{3+}. The substitution of Ce^{4+} for La^{3+} brings Co^{2+} ions to Co^{3+} matrix. Co^{2+} always shows a high-spin state, HS, $t_{2g}^5e_g^0$, while Co^{3+} shows a low-spin state, LS, t_{2g}^6, and intermediate-spin state, IS, $t_{2g}^5e_g^1$ (see the inset of Figure 6). As the temperature increases, the LS−IS transition takes place, which result in the delocalization and hopping of the e_g electron between HS Co^{2+} and IS Co^{3+} due to the degenerate configurations of HS Co^{2+} and IS Co^{3+}. This transition destroys the spin blockade effect and induces an abrupt decrease of resistivity as well as an insulator−metal transition. Meanwhile, the changes in thermopower and thermal conductivity are moderate. As a result, a maxmum of figure of merit ZT is present at the transition temperature.

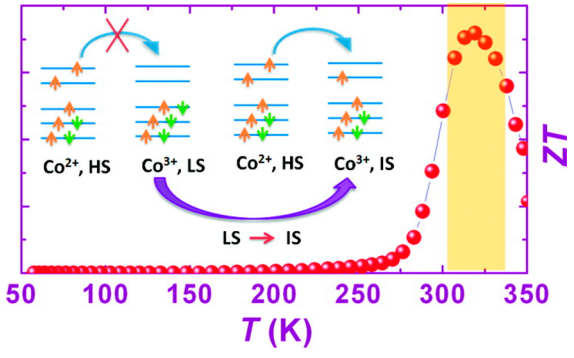

Figure 6. Temperature-dependent ZT values of $La_{0.94}Ce_{0.06}CoO_3$. The inset is the sketch of the e_g electron hopping processes between HS Co^{2+} and LS Co^{3+}, and between HS Co^{2+} and IS Co^{3+}. Adapted with permission from ref 32. Copyright 2010 American Chemical Society.

2.3. Superionic Conductor with Disordered Structure

The concept of a "phonon glass electron crystal" (PGEC) proposed by Glen Slack in the mid-1990s,[33] which idealistically possesses both high electrical conductivity like a crystal and low thermal conductivity like a glass, was theorized to be the most influential principle to guide high performance thermoelectric materials research in the past 20 years. Although this idea spurred a significant amount of research in complex materials systems such as skutterudites,[34−37] Zintl phases,[38,39] and clathrates,[40−43] the perfect PGEC material has yet to be synthesized.[44] Beyond these traditional materials, thanks to their strong short-wavelength phonon scattering causing ultralow thermal conductivity, those materials with disordered structure have long been considered as promising candidates for high-performance thermoelectric materials.[45,46] However, at the same time, in common disordered structures, the local potential energy fluctuations induce additional charge carrier scattering resulting in mobility reduction as well, which results in reduced electrical conductivity.

As typical disordered systems, compared with ordinary disordered structures, superionic conductors show the greatest advantage of high mobility of cations or anions in the lattice, which significantly minimize the thermal conductivity with no deteriorated electrical conductivity for improving thermoelectric properties.[47,48] For example, at high temperature, the Se atoms in $Cu_{2-x}Se$ form a rigid face-centered cubic sublattice, providing a crystalline pathway for semiconducting electrons (or more precisely holes); the copper ions are highly disordered around the Se sublattice and are superionic with liquid-like mobility, which results in the high ZT value of 1.5 at 1000 K (as seen in Figure 7).[47] This extraordinary "liquid-like" behavior enables superionic conductors to be excellent thermoelectric

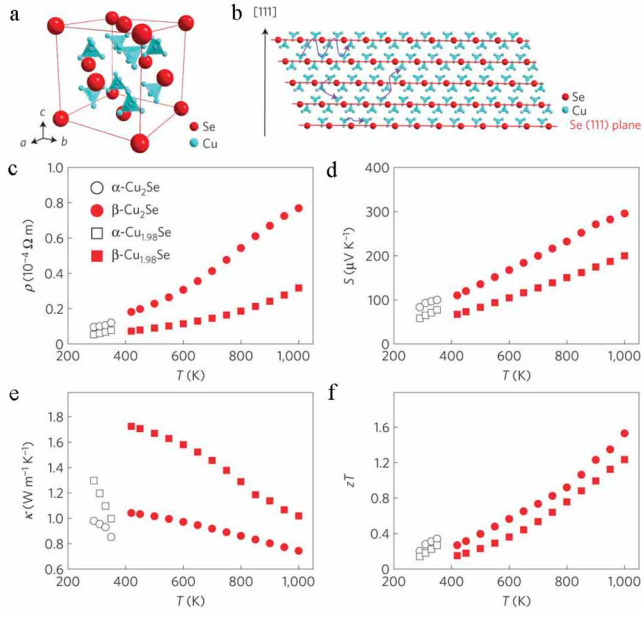

Figure 7. (a, b) Crystal structure of $Cu_{2-x}Se$ at high temperatures. (c−f) Thermoelectric properties of the $Cu_{2-x}Se$: temperature-dependent electrical resistivity (c), thermopower S (d), thermal conductivity (e), and ZT values (f). Adapted with permission from ref 47. Copyright 2012 Nature Publishing Group.

dx.doi.org/10.1021/ar400290f | Acc. Chem. Res. 2014, 47, 1287−1295

materials, which indicates a new strategy and direction for high-efficiency thermoelectric materials by exploring systems where there exists a crystalline sublattice for electronic conduction surrounded by liquid-like ions.

However, the superionic states with intrinsic high electrical conductivity and low thermal conductivity usually can only be achieved at high temperature, at which they should often experience the phase transition. For example, above-mentioned $AgBiSe_2$ shows a high ZT value of 1.5 at 700 K due to the high electric conductivity and low thermal conductivity, which are derived from the high mobility of fully disordered Ag/Bi bimetal ions in the Se NaCl-type sublattice. However, the excellent thermoelectric performance existing only at high temperatures greatly limits the practical working temperature. Therefore, stabilization of the high temperature superionic states to low even room temperature should be desirable for broadening the working temperature range as excellent thermoelectric materials. The formation of solid solution is a widespread adopted strategy to alter the phase transition temperature,[49] through which we stabilize the nonambient disordered state to room temperature.[50] In addition, we introduce the in situ formed homojunctions on the surface of solid-solutioned nanoplates, which not only overcome the electrical conductivity deterioration induced by the heterogeneous composition in heterojunctions but also further reduce the thermal conductivity by the enhanced midwavelength phonon scattering. These findings reveal that the formation of a solid solution coupled with homojunctions in a superionic conductor allows synergistically much enhanced thermoelectric properties through the significant reduction of thermal conductivity with no deteriorated electrical conductivity, which may conform to the "PGEC" approach (as seen in Figure 8).

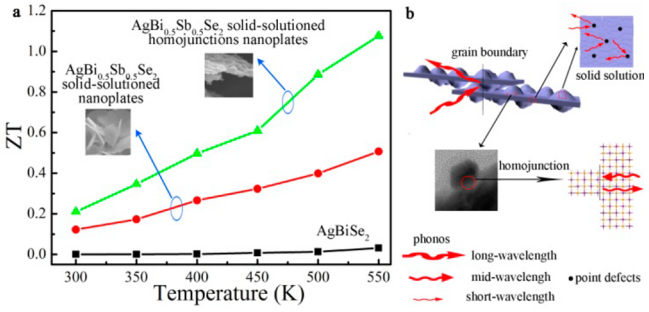

Figure 8. (a) The thermoelectric properties of $AgBi_{0.5}Sb_{0.5}Se_2$ solid-solution homojunction nanoplates and (b) schematic diagram illustrating various phonon scattering mechanisms in $AgBi_{0.5}Sb_{0.5}Se_2$ solid-solutioned homojunction nanoplates. Adapted with permission from ref 50. Copyright 2012 American Chemical Society.

3. FULL DECOUPLING OF THREE PARAMETERS

As mentioned above, the strongly interrelated thermoelectric parameters have been regarded as one of the biggest bottlenecks to obtain high-performance thermoelectric materials. Therefore, it is the ultimate goal to fully decouple these three parameters to synergistically optimize the thermoelectric performance, despite many strategies verifying that one can decouple the power factor and thermal conductivity based on the reduction of lattice thermal conductivity. In the following section, we will discuss our long time efforts in this challenging field in detail.

3.1. Spin Entropy in Wide-Gap Semiconductors

On the basis of the thermodynamic analysis, we can conclude that the thermopower is proportional to the average flux of entropy carried by each charge carrier,[51] which indicates that any entropy current density carried by thermal or electronic factors should be taken into account for the improvement of thermoelectric performance. In fact, in addition to the charge carriers (electrons and holes) and phonons, it has been proven that the electron spin and orbital can also carry entropy current that is responsible for the coexistence of high thermopower and electrical conductivity.[52−54] For example, in the case of cobaltite oxides, the spin entropy of Co ions gives it large thermopower, an order of magnitude higher than the common metal and high-temperature superconductors, which results in a high ZT value of 0.8 at high temperature and breaks through the old concept that oxide compounds are unsuitable for thermoelectric materials. Recently, we also propose to disentangle of the otherwise interconnected quantities through the new source of entropy from the degree of freedom 3d electrons in the magnetic ions, that is, spin, which is further facilitated by narrowed band gap and stronger anharmonic coupling for improving all the prerequisites of ZT: larger Seebeck coefficient, higher electrical conductivity, and lower thermal conductivity.[55] This idea is experimentally achieved in quaternary chalcogenide nanocrystals, a type of wide band gap semiconductor, in particular, $I_2-II-IV-VI_4$ adamantines, which have been recently found to be potentially thermoelectric materials, since their distorted chalcopyrite-like structures endow them with low lattice thermal conductivities. Therefore, this family of semiconductors provides an ideal platform to explore the independent control of Seebeck coefficient and electrical and thermal conductivity, which is the long sought best strategy to develop thermoelectric materials with extraordinary energy conversion efficiency. For example (as seen in Figure 9), the ZT value of the Ni^{2+} ion doped

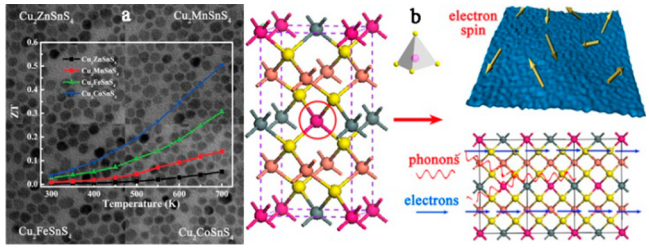

Figure 9. (a) Temperature-dependent thermoelectric figure of merit ZT for Cu_2XSnS_4 nanocrystals. (b) Schematic diagram illustrating various electron spin and phonon scattering in magnetic ion fully substituted quaternary nanocrystals. Adapted with permission from ref 55. Copyright 2014 Royal Society of Chemistry.

Cu_2ZnSnS_4 nanocrystal is extraordinarily enhanced by 7.4 times compared with that of pure Cu_2ZnSnS_4 nanocrystals, while the fully Co^{2+} substituted Cu_2CoSnS_4 nanocrystal shows a 9.2 times improvement in the ZT value.

3.2. Atomically Thick Nanosheets with Two-Dimenional Electron Gas

Since Hicks and Dresselhaous first predicted that the thermoelectric performance can be significantly enhanced in a superlattice quantum well due to the peculiar electronic structure far beyond what was believed impossible in bulk materials, the improvement of thermoelectric properties

dx.doi.org/10.1021/ar400290f | Acc. Chem. Res. 2014, 47, 1287−1295

through nanostructure has been one of the most important improvements in the thermoelectric materials research field.[56] The most exciting characteristic of electronic in superlattices is the two-dimensional electron gas (2DEG), which confines the electrons to moving in the direction parallel to the surface resulting in the quantization of energy in the perpendicular direction. The presence of two-dimensional electron gas makes the superlattice possess a large number of interfaces and periodic structure, which is beneficial to increase the energy state density near the Fermi level and greatly improve the Seebeck coefficient.[57,58] Meanwhile, the superlattice also exhibits high electrical conductivity in the direction parallel to the surface due to the high carrier concentration and mobility in this confined direction.[59]

With respect to those distinctive advantages of superlattice, Ohta et al. has reported a giant Seebeck coefficient and thermoelectric power factor in the confined two-dimensional electron gas. They fabricated $SrTiO_3/SrTi_{1-x}Nb_xO_3$ and $TiO_2/SrTiO_3$ superlattice systems through pulse laser deposition, which both show the expected large thermopower and high electrical conductivity resulting in the extraordinary thermoelectric performance at room temperature (as seen in Figure 10).[60,61] The enhanced ZT value in the superlattice thin film

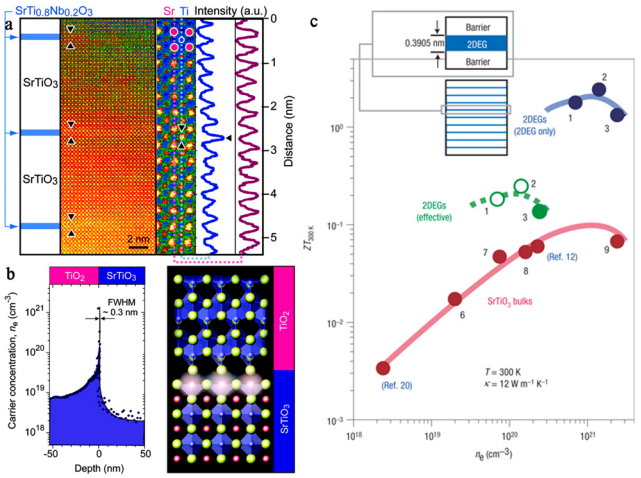

Figure 10. (a) High-angle annular dark-field scanning transmission electron microscope image and Ti-$L_{2,3}$ edge electron energy loss spectroscopy profile of $SrTiO_3/SrTi_{1-x}Nb_xO_3$ superlattice. (b) Depth profile across the heterointerface between a TiO_2 epitaxial layer and the $SrTiO_3$ substrate, and schematic drawing of the heterointerface crystal structure. (c) Figures of merit, ZT, of the 2DEGs and the $SrTiO_3$-bulk samples as a function of carrier concentration at room temperature. Panels a and c were adapted with permission from ref 60. Copyright 2007 Nature Publishing Group. Panel b was adapted with permission from ref 61. Copyright 2008 American Chemical Society.

has also been widely confirmed in the subsequent experiments in many other systems. However, superlattice thin films fabricated by atomic layer deposition (ALD) or pulse laser deposition (PLD) techniques are not easily incorporated into commercial devices, since they are too slow and expensive to fabricate,[62] and they cannot be fabricated in sufficient quantities, which strongly hinder the commercialization of superlattice thermoelectric materials.

Recently, we develop anew concept based on an ultrathin-nanosheet-based composite fabricated from atomically thick nanosheets for decoupled optimization of the thermoelectric parameters to improve thermoelectric performance.[63] Taking Bi_2Se_3 as an example, one of the most widely used thermoelectric materials with strong 2DEG perpendicular to *c*-axis, we synthesized ultrathin Bi_2Se_3 nanosheets with thickness near to atomic thickness via a scalable intercalation/exfoliation strategy. The nanosheets were were then fabricated to a single-layer-based (SLB) composite through layer-by-layer assembly, cold-press, and sintering. This SLB composite retains the original strong 2DEG, which results in significantly enhanced thermopower and electrical conductivity. Meanwhile, the surface distortion in the atomically thick nanosheet, revealed by the synchrotron-radiation X-ray absorption fine structure (srXAFS) spectra, and adequate grain boundaries strongly scatter the whole wavelength photons rather than electrons, which guarantees reduced thermal conductivities with a minimal detrimental effect on the electrical properties. As a result, the SLB composite achieved a ZT value of 0.35 at 400 K, which is ca. 8 times higher than that of the bulk material (as seen in Figure 11).

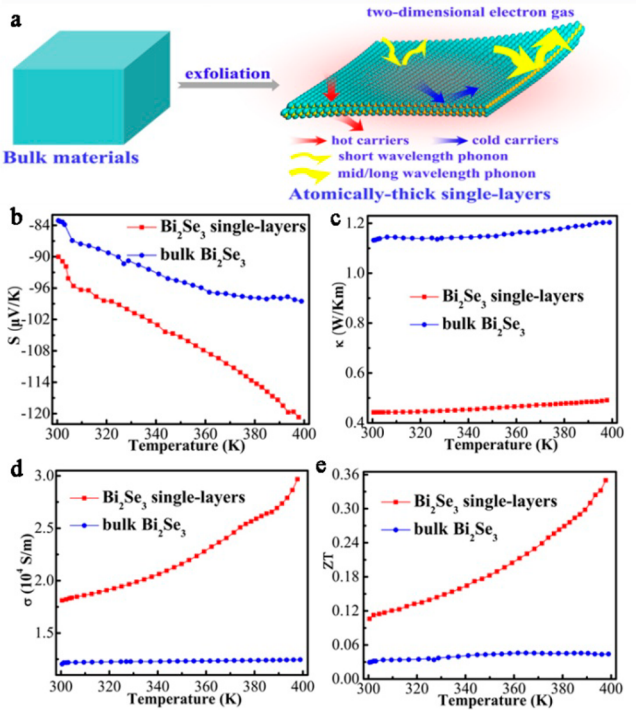

Figure 11. (a) Schematic representation for the transport properties of Bi_2Se_3 single layer. (b–e) Thermoelectric properties of the bulk and single layered Bi_2Se_3: temperature dependences of thermopower *S* (b), thermal conductivity (c), electrical resistivity (d), and ZT values (e). Adapted with permission from ref 63. Copyright 2012 American Chemical Society.

4. CONCLUSION AND OUTLOOK

As a clean and renewable energy source, thermoelectric materials are expected to play an important role in waste heat or automotive exhaust power generation, space technology, environmentally friendly refrigerators, high-precision temperature control systems, and other aspects, which have attracted considerable attention among physics, chemistry, and materials researchers to understand this field thoroughly in the past few years. Compared with 10 years ago, a diverse array of new approaches, from complexity within the unit cell to nanostructured bulk materials, have all led to enhanced-efficiency

materials. However, several issues and challenges still exist, for example, ZT > 3 is yet to be achieved. Therefore, exploring novel thermoelectric materials achieving synergistic or even decoupling modulation of the three thermoelectrical parameters, in addition to the optimization of materials' intrinsic electronic structure, is of great importance to overcome the constraints of low conversion efficiency on the large-scale applicaton.

In this Account, we outline our recently developed new strategies to decouple the thermoelectric parameters for synergistic optimization of thermoelectric performance, including utilizing phase transition and superionic conductors with disordered structure to decouple the power factor and thermal conductivity. Most exciting, both the creation of spin entropy in wide-gap semiconductors and the fabrication of an ultrathin-nanosheet-based composite with 2D electron gas preliminarily realized the decoupling optimization of three parameters. From our own and other research groups' results, we envision that the proper choice of nanostructured materials with intrinsic characteristics, in their bulk counterpart, such as phase transition and so on, could be a general route to decouple the strongly interrelated parameters for significantly enhanced thermoelectric performance. All of these approaches are decided from materials synthesis and characterization to understand the underlying physical and chemical mechanisms, which require collaborations between chemists, physicists, and materials scientists.

Overall, the global need for sustainable energy coupled with the recent advances in thermoelectrics inspires a growing excitement in this field, but there is still much work to be done in this area before materials with the high thermoelectric figure-of-merit necessary for wide applications are found or created. We are hopeful and optimistic that progress continued at the pace of the past 10 years will lead to additional large leaps in the thermoelectric figure of merit.

AUTHOR INFORMATION

Corresponding Author

*E-mail: yxie@ustc.edu.cn.

Funding

This work was financially supported by National Natural Science Foundation of China (Grants 11079004, 90922016, 21331005, and 11321503), Chinese Academy of Science (Grant XDB01020300), and the Fundamental Research Funds for the Central University (Grant WK 2060190020).

Notes

The authors declare no competing financial interest.

Biographies

Chong Xiao is a postdoctoral researcher in Collaborative Innovation Center of Chemistry for Energy Materials, University of Science and Technology of China. He received his Ph.D. degree from University of Science and Technology of China under the supervision of Prof. Yi Xie. He has been working on advanced thermoelectric semiconductors, especially nano-thermoelectric materials with synergistically optimized electrical and thermal transport, more than four years, from materials synthesis and characterization to understanding the underlying physics and chemistry mechanisms.

Zhou Li is a graduate student in University of Science and Technology of China under the supervision of Prof. Yi Xie. He received his B.S. degree in Material Physics from Wuhan University of Technology in 2012. Currently, his research interest is focused on the synthesis and characterization of high-performance thermoelectric materials.

Kun Li received his B.S. degree of natural science chemistry from University of Science and Technology of China in 2013. Then he joined Prof. Yi Xie's group as a graduate student. His research interests include synthesis of nanostructured materials and exploration of novel thermoelectric materials.

Pengcheng Huang received his B.S. degree in Chemistry from University of Science and Technology of China. He joined Prof. Yi Xie's group as a graduate student in 2013. His research interests focus on the synthesis and utilization of nanostructured materials for thermoelectric applications.

Yi Xie received her B.S. degree from Xiamen University (1988) and a Ph.D. from the University of Science and Technology of China (USTC, 1996). She is now a Principal Investigator of Hefei National Laboratory for Physical Sciences at the Microscale and a full professor of the Department of Chemistry, USTC. She was appointed as the Cheung Kong Scholar Professor of inorganic chemistry in 2000 and also is a recipient of many awards, including the Chinese National Nature Science Award (2001 and 2012), China Young Scientist Award (2002), China Young Female Scientist Award (2006), and IUPAC Distinguished Women in Chemistry/Chemical Engineering Award (2013). Her research interests are cutting-edge research at four major frontiers: solid state materials chemistry, nanotechnology, energy science, and theoretical physics.

REFERENCES

(1) Wise, M.; Calvin, K.; Thomson, A.; Clarke, L.; Bond-Lamberty, B.; Sands, R.; Smith, S. J.; Janetos, A.; Edmonds, J. Implications of Limiting CO_2 Concentrations for Land Use and Energy. *Science* **2009**, *324*, 1183−1186.

(2) Wheeler, T.; Braun, J. Climate Change Impacts on Global Food Security. *Science* **2013**, *341*, 508−513.

(3) Sales, B. C.; Mandrus, D.; Williams, R. K. Filled Skutterudite Antimonides: A New Class of Thermoelectric Materials. *Science* **1996**, *272*, 1325−1328.

(4) Chung, D. Y.; Hogan, T.; Brazis, P.; Rocci-Lane, M.; Kannewurf, C.; Bastea, M.; Uher, C.; Kanatzidis, M. G. CsBi4Te6 A High-Performance Thermoelectric Material for Low-Temperature Applications. *Science* **2000**, *287*, 1024−1027.

(5) Harman, T. C.; Taylor, P. J.; Walsh, M. P.; LaForge, B. E. Quantum Dot Superlattice Thermoelectric Materials and Devices. *Science* **2002**, *297*, 2229−2232.

(6) Majumdar, A. Thermoelectricity in Semiconductor Nanostructures. *Science* **2004**, *303*, 777−778.

(7) Hsu, K. F.; Loo, S.; Guo, F.; Chen, W.; Dyck, J. S.; Uher, C.; Hogan, T.; Polychroniadis, E. K.; Kanatzidis, M. G. Cubic $AgPb_mSbTe_{2+m}$ Bulk Thermoelectric Materials with High Figure of Merit. *Science* **2004**, *303*, 818−821.

(8) Heremans, J. P.; Jovovic, V.; S. Toberer, E.; Saramat, A.; Kurosaki, K.; Charoenphakdee, A.; Yamanaka, S.; Snyder, G. J. Enhancement of Thermoelectric Efficiency in PbTe by Distortion of the Electronic Density of States. *Science* **2008**, *321*, 554−557.

(9) Poudel, B.; Hao, Q.; Ma, Y.; Lan, Y. C.; Minnich, A.; Yu, B.; Yan, X.; Wang, D. Z.; Muto, A.; Vashaee, D.; Chen, X. Y.; Liu, J. M.; Dresselhaus, M. S.; Chen, G.; Ren, Z. F. High-Thermoelectric Performance of Nanostructured Bismuth Antimony Telluride Bulk Alloys. *Science* **2008**, *320*, 634−638.

(10) Bell, L. E. Cooling, Heating, Generating Power, and Recovering Waste Heat with Thermoelectric Systems. *Science* **2008**, *321*, 1457−1461.

(11) Hochbaum, A. I.; Chen, R. K.; Delgado, R. D.; Liang, W. J.; Garnett, E. C.; Najarian, M.; Majumdar, A.; Yang, P. D. Enhanced Thermoelectric Performance of Rough Silicon Nanowires. *Nature* **2008**, *451*, 163−167.

(12) Pei, Y. Z.; Shi, X. Y.; LaLonde, A.; Wang, H.; Chen, L. D.; Snyder, G. J. Convergence of Electronic Bands for High Performance Bulk Thermoelectric. *Nature* **2011**, *473*, 66−69.
(13) Biswas, K.; He, J. Q.; Blum, I. D.; Wu, C.-I.; Hogan, T. P.; Seidman, D. N.; Dravid, V. P.; Kanatzidis, M. G. High-Performance Bulk Thermoelectrics with All-Scale Hierarchical Architectures. *Nature* **2012**, *489*, 414−418.
(14) Snyder, G. J.; Toberer, E. S. Complex Thermoelectric Materials. *Nat. Mater.* **2008**, *7*, 105−114.
(15) Shakouri, A. Recent Developments in Semiconductor Thermoelectric Physics and Materials. *Annu. Rev. Mater. Res.* **2011**, *41*, 399−431.
(16) Mahan, G. D.; Bartkowiak, M. Wiedemann-Franz Law at Boundaries. *Appl. Phys. Lett.* **1999**, *74*, 953−954.
(17) Tritt, T. M. Thermoelectric Phenomena, Materials, and Applications. *Annu. Rev. Mater. Res.* **2011**, *41*, 433−448.
(18) Rao, C. N. R. Phase Transitions and the Chemistry of Solids. *Acc. Chem. Res.* **1984**, *17*, 83−89.
(19) Imada, M.; Fujimori, A.; Tokura, Y. Metal-Insulator Transitions. *Rev. Mod. Phys.* **1998**, *70*, 1039−1263.
(20) Wu, C. Z.; Feng, F.; Feng, J.; Dai, J.; Peng, L. L.; Zhao, J. Y.; Yang, J. L.; Si, C.; Wu, Z. Y.; Xie, Y. Hydrogen-Incorporation Stabilization of Metallic VO_2(R) Phase to Room Temperature, Displaying Promising Low-Temperature Thermoelectric Effect. *J. Am. Chem. Soc.* **2011**, *133*, 13798−13801.
(21) Grinolds, M. S.; Lobastov, V. A.; Weissenrieder, J.; Zewail, A. H. Four-Dimensional Ultrafast Electron Microscopy of Phase Transitions. *Proc. Nat. Acad. Sci. U. S. A.* **2006**, *103*, 18427−18431.
(22) Wu, C. Z.; Feng, F.; Xie, Y. Design of Vanadium Oxide Structures with Controllable Electrical Properties for Energy Applications. *Chem. Soc. Rev.* **2013**, *42*, 5157−5183.
(23) Schoen, D. T.; Xie, C.; Cui, Y. Electrical Switching and Phase Transformation in Silver Selenide Nanowires. *J. Am. Chem. Soc.* **2007**, *129*, 4116−4117.
(24) In, J.; Yoo, Y.; Kim, J.-G.; Seo, K.; Kim, H.; Ihee, H.; Oh, S. H.; Kim, B. In Situ TEM Observation of Heterogeneous Phase Transition of a Constrained Single-Crystalline Ag_2Te Nanowire. *Nano Lett.* **2010**, *10*, 4501−4504.
(25) Jang, J.; Pan, F.; Braam, K.; Subramanian, V. Resistance Switching Characteristics of Solid Electrolyte Chalcogenide Ag_2Se Nanoparticles for Flexible Nonvolatile Memory Applications. *Adv. Mater.* **2012**, *24*, 3573−3576.
(26) Billetter, H.; Ruschewitz, U. Structural Phase Transition in Ag2Se (Naumannite). *Z. Anorg. Allg. Chem.* **2008**, *634*, 241−246.
(27) Xiao, C.; Xu, J.; Li, K.; Feng, J.; Yang, J. L.; Xie, Y. Superionic Phase Transition in Silver Chalcogenide Nanocrystals Realizing Optimized Thermoelectric Performance. *J. Am. Chem. Soc.* **2012**, *134*, 4287−4293.
(28) Liu, H. H.; Yuan, X.; Lu, P.; Shi, X.; Xu, F. F.; He, Y.; Tang, Y. S.; Bai, S. Q.; Zhang, W. Q.; Chen, L. D.; Lin, Y.; Shi, L.; Lin, H.; Gao, X. Y.; Zhang, X. M.; Chi, H.; Uher, C. Ultrahigh Thermoelectric Performance by Electron and Phonon Critical Scattering in $Cu_2Se_{1-x}I_x$. *Adv. Mater.* **2013**, *25*, 6607−6612.
(29) Xiao, C.; Qin, X. M.; Zhang, J.; An, R.; Xu, J.; Li, K.; Cao, B. X.; Yang, J. L.; Ye, B. J.; Xie, Y. High Thermoelectric and Reversible *p-n-p* Conduction Type Switching Integrated in Di-metal Chalcogenide. *J. Am. Chem. Soc.* **2012**, *134*, 18460−18466.
(30) Manolikas, C.; Spyridelis, J. Electron Microscopic Study of Polymorphism and Defects in $AgBiSe_2$ and $AgBiS_2$. *Mater. Res. Bull.* **1977**, *12*, 907−913.
(31) Larson, P.; Mahanti, S. D. Prediction of Semiconducting and Metallic Behavior in $AgBiSe_2$ due to Structural Change. Presented at the American Physical Society, Annual March Meeting, March 12−16, 2001.
(32) Wang, Y.; Sui, Y.; Wang, X. J.; Su, W. H.; Cao, W. W.; Liu, X. Y. Thermoelectric Response Driven by Spin-State Transition in $La_{1-x}Ce_xCoO_3$ Perovskites. *ACS Appl. Mater. Interfaces* **2010**, *2*, 2213−2217.
(33) Slack, G. A. In *CRC Handbook of Thermoelectrics*; Rowe, D. M., Ed.; CRC: Boca Raton, FL, 1995; pp 407−440.
(34) Koza, M. M.; Johnson, M. R.; Viennois, R.; Mutka, H.; Girard, L.; Ravot, D. Breakdown of Phonon Glass Paradigm in La- and Ce-Filled Fe_4Sb_{12} Skutterudites. *Nat. Mater.* **2008**, *7*, 805−810.
(35) Zhao, W. Y.; Wei, P.; Zhang, Q. J.; Dong, C. L.; Liu, L. S.; Tang, X. F. Enhanced Thermoelectric Performance in Barium and Indium Double-Filled Skutterudite Bulk Materials via Orbital Hybridization Induced by Indium Fille. *J. Am. Chem. Soc.* **2009**, *131*, 3713−3720.
(36) Shi, X.; Yang, J.; Salvador, J. R.; Chi, M. F.; Cho, J. Y.; Wang, H.; Bai, S. Q.; Yang, J. H.; Zhang, W. Q.; Chen, L. D. Multiple-Filled Skutterudites: High Thermoelectric Figure of Merit through Separately Optimizing Electrical and Thermal Transports. *J. Am. Chem. Soc.* **2011**, *133*, 7837−7846.
(37) Schmokel, M. S.; Bjerg, L.; Overgaard, J.; Larsen, F. K.; Madsen, G. K. H.; Sugimoto, K.; Takata, M.; Iversen, B. B. Pushing X-ray Electron Densities to the Limit: Thermoelectric $CoSb_3$. *Angew. Chem., Int. Ed.* **2013**, *52*, 1503−1506.
(38) Snyder, G. J.; Christensen, M.; Nishibori, E.; Caillat, T.; Iversen, B. B. Disordered Zinc in Zn_4S_{b3} with Phonon-Glass and Electron-Crystal Thermoelectric Properties. *Nat. Mater.* **2004**, *3*, 458−463.
(39) Nylen, J.; Andersson, M.; Lidin, S.; Haussermann, U. The Structure of α-Zn_4Sb_3: Ordering of the Phonon-Glass Thermoelectric Material β-Zn_4Sb_3. *J. Am. Chem. Soc.* **2004**, *126*, 16306−16307.
(40) Guloy, A. M.; Ramlau, R.; Tang, Z. J.; Schnelle, W.; Baitinger, M.; Grin, Y. A Guest-Free Germanium Clathrate. *Nature* **2006**, *443*, 320−323.
(41) Christensen, M.; Lock, N.; Overgaard, J.; Iversen, B. B. Crystal Structures of Thermoelectric n- and p-type $Ba_8Ga_{16}Ge_{30}$ Studied by Single Crystal, Multitemperature, Neutron Diffraction, Conventional X-ray Diffraction and Resonant Synchrotron X-ray Diffraction. *J. Am. Chem. Soc.* **2006**, *128*, 15657−15665.
(42) Christensen, M.; Abrahamsen, A. B.; Christensen, N. B.; Juranyi, F.; Andersen, N. H.; Lefmann, K.; Andreasson, J.; Bahl, C. R. H.; Iversen, B. B. Avoided Crossing of Rattler Modes in Thermoelectric Materials. *Nat. Mater.* **2008**, *7*, 811−815.
(43) Liu, Y.; Wu, L. M.; Li, L. H.; Du, S. W.; Corbett, J. D.; Chen, L. The Antimony-Based Type I Clathrate Compounds $Cs_8Cd_{18}Sb_{28}$ and $Cs_8Zn_{18}Sb_{28}$. *Angew. Chem., Int. Ed.* **2009**, *48*, 5305−5308.
(44) Sabah, K. B.; Fleurial, J. P.; Richard, B. K. Nanostructured Materials for Thermoelectric Applications. *Chem. Commun.* **2010**, *46*, 8311−8324.
(45) Morelli, D. T.; Jovovic, V.; Heremans, J. P. Intrinsically Minimal Thermal Conductivity in Cubic I-V-VI_2 Semiconductors. *Phys. Rev. Lett.* **2008**, *101*, No. 035901.
(46) Wang, H.; LaLonde, A. D.; Pei, Y. Z.; Snyder, G. J. The Criteria for Beneficial Disorder in Thermoelectric Solid Solutions. *Adv. Funct. Mater.* **2013**, *23*, 1586−1596.
(47) Liu, H. L.; Shi, X.; Xu, F. F.; Zhang, L. L.; Zhang, W. Q.; Chen, L. D.; Li, Q.; Uher, C.; Day, T.; Snyder, G. J. Copper Ion Liquid-Like Thermoelectric. *Nat. Mater.* **2012**, *11*, 422−425.
(48) Yu, B.; Liu, W. S.; Chen, S.; Wang, H.; Wang, H. Z.; Chen, G.; Ren, Z. F. Thermoelectric Properties of Copper Selenide with Ordered Selenium Layer and Disordered Copper Layer. *Nano Energy* **2012**, *1*, 472−478.
(49) Whittaker, L.; Wu, T. L.; Stabile, A.; Sambandamurthy, G.; Banerjee, S. Single-Nanowire Raman Microprobe Studies of Doping-, Temperature-, and Voltage-Induced Metal-Insulator Transitions of $W_xV_{1-x}O_2$ Nanowires. *ACS Nano* **2011**, *5*, 8861−8867.
(50) Xiao, C.; Xu, J.; Cao, B. X.; Li, K.; Kong, M. G.; Xie, Y. Solid-Solutioned Homojunction Nanoplates with Disordered Lattice: A Promising Approach toward "Phonon Glass Electron Crystal" Thermoelectric Materials. *J. Am. Chem. Soc.* **2012**, *134*, 7971−7977.
(51) Wood, C. Materials for Thermoelectric Energy Conversion. *Rep. Prog. Phys.* **1988**, *51*, 459−539.
(52) Wang, Y. Y.; Rogado, N. S.; Cava, R. J.; Ong, N. P. Spin Entropy As the Likely Source of Enhanced Thermopower in $Na_xCo_2O_4$. *Nature* **2003**, *423*, 425−428.

(53) Koshibae, W.; Maekawa, S. Effects of Spin and Orbital Degeneracy on the Thermopower of Strongly Correlated Systems. *Phys. Rev. Lett.* **2001**, *87*, No. 236603.
(54) Klie, R. F.; Qiao, Q.; Paulauskas, T.; Gulec, A.; Rebola, A.; Ogut, S.; Prange, M. P.; Idrobo, J. C.; Pantelides, S. T.; Kolesnik, S.; Dabrowski, B.; Ozdemir, M.; Boyraz, C.; Mazumdar, D.; Gupta, A. Observations of Co^{4+} in a Higher Spin State and the Increase in the Seebeck Coefficient of Thermoelectric $Ca_3Co_4O_9$. *Phys. Rev. Lett.* **2012**, *108*, No. 196601.
(55) Xiao, C.; Li, K.; Zhang, J. J.; Tong, W.; Liu, Y. W.; Li, Z.; Huang, P. C.; Pan, B. C.; Su, H. B.; Xie, Y. Magnetic Ions in Wide Band Gap Semiconductor Nanocrystals for Optimized Thermoelectric Properties. *Mater. Horiz.* **2014**, *1*, 81−86.
(56) Hicks, L. D.; Dresselhaus, M. S. The Effect of Quantum Well Structures on the Thermoelectric Figure of Merit. *Phys. Rev. B* **1993**, *47*, 12727−12731.
(57) Vineis, C. J.; Shakouri, A.; Majumdar, A.; Kanatzidis, M. G. Nanostructured Thermoelectrics: Big Effi ciency Gains from Small Features. *Adv. Mater.* **2010**, *22*, 3970−3980.
(58) Takei, K.; Madsen, M.; Fang, H.; Kapadia, R.; Chuang, S.; Kim, H. S.; Liu, C.; Plis, E.; Nah, J.; Krishna, S.; Chueh, Y.; Guo, J.; Javey, A. Nanoscale InGaSb Heterostructure Membranes on Si Substrates for High Hole Mobility Transistors. *Nano Lett.* **2012**, *12*, 2060−2066.
(59) Venkatasubramanian, R.; Siivola, E.; Colpitts, T.; O'Quinn, B. Thin-Film Thermoelectric Devices with High Room-Temperature Figures of Merit. *Nature* **2001**, *413*, 597−602.
(60) Ohta, H.; Kim, S.; Mune, Y.; Mizoguchi, T.; Nomura, K.; Ohta, S.; Nakanishi, Y.; Ikuhara, Y.; Hirano, M.; Hosono, H.; Koumoto, K. Giant Thermoelectric Seebeck Coefficient of a Two-Dimensional Electron Gas in $SrTiO_3$. *Nat. Mater.* **2007**, *6*, 129−134.
(61) Ohta, H.; Sugiura, K.; Koumoto, K. Recent Progress in Oxide Thermoelectric Materials *p*-type $Ca_3Co_4O_9$ and *n*-type $SrTiO_3$. *Inorg. Chem.* **2008**, *47*, 8429.
(62) Garcia-Martin, S.; King, G.; Urones-Garrote, E.; Nénert, G.; Woodward, P. M. Spontaneous Superlattice Formation in the Doubly Ordered Perovskite $KLaMnWO_6$. *Chem. Mater.* **2011**, *23*, 163−170.
(63) Sun, Y. F.; Cheng, H.; Gao, S.; Liu, Q. H.; Sun, Z. H.; Xiao, C.; Wu, C. Z.; Wei, S. Q.; Xie, Y. Atomically Thick Bismuth Selenide Freestanding Single Layers Achieving Enhanced Thermoelectric Energy Harvesting. *J. Am. Chem. Soc.* **2012**, *134*, 20294−20297.